NIH Public Access
Author Manuscript
J Neurochem. Author manuscript; available in PMC 2010 August 1.

Published in final edited form as:
J Neurochem. 2009 August ; 110(4): 1191–1202. doi:10.1111/j.1471-4159.2009.06202.x.

SPHINGOSINE-1-PHOSPHATE RECEPTORS MEDIATE NEUROMODULATORY FUNCTIONS IN THE CNS

Laura J. Sim-Selley[1], **Paulette B. Goforth**[5], **Mba U. Mba**[1], **Timothy L. Macdonald**[4], **Kevin R. Lynch**[3], **Sheldon Milstien**[2], **Sarah Spiegel**[2], **Leslie S. Satin**[5], **Sandra P. Welch**[1], and **Dana E. Selley**[1]

[1]Department of Pharmacology and Toxicology and Institute for Drug and Alcohol Studies, Virginia Commonwealth University School of Medicine, Richmond, Virginia 23298

[2]Department of Biochemistry and Molecular Biology, Virginia Commonwealth University School of Medicine, Richmond, Virginia 23298

[3]Department of Pharmacology, University of Virginia School of Medicine, Charlottesville, VA, 22908

[4]Department of Chemistry, University of Virginia, Charlottesville, VA, 22903

Abstract

Sphingosine-1-phosphate is a ubiquitous, lipophilic cellular mediator that acts in part by activation of G-protein-coupled receptors. Modulation of S1P signaling is an emerging pharmacotherapeutic target for immunomodulatory drugs. Although multiple S1P receptor types exist in the CNS, little is known about their function. Here we report that S1P stimulated G- protein activity in the CNS, and results from [^{35}S]GTPγS autoradiography using the $S1P_1$-selective agonist SEW2871 and the $S1P_{1/3}$-selective antagonist VPC44116 show that in several regions a majority of this activity is mediated by $S1P_1$ receptors. S1P receptor activation inhibited glutamatergic neurotransmission as determined by electrophysiological recordings in cortical neurons *in vitro*, and this effect was mimicked by SEW2871 and inhibited by VPC44116. Moreover, central administration of S1P produced *in vivo* effects resembling the actions of cannabinoids, including thermal antinociception, hypothermia, catalepsy and hypolocomotion, but these actions were independent of CB_1 receptors. At least one of the central effects of S1P, thermal antinociception, is also at least partly $S1P_1$ receptor mediated because it was produced by SEW2871 and attenuated by VPC44116. These results indicate that CNS S1P receptors are part of a physiologically relevant and widespread neuromodulatory system, and that the $S1P_1$ receptor contributes to S1P-mediated antinociception.

Keywords

S1P receptor; GPCR; Glutamate; Analgesia; Hypothermia; Autoradiography

INTRODUCTION

Cellular lysolipids are important in cell-cell communication and the field is rapidly growing. These important cellular mediators include sphingosine-1-phosphate (S1P),

Corresponding Author: Dr. Laura Sim-Selley Dept. of Pharmacology and Toxicology, Box 980524, 1112 East Clay St. Virginia Commonwealth University School of Medicine, Richmond, Virginia 23298 Phone: 804-827-0464, FAX: 804-828-1532, email: lisimsel@vcu.edu.
[5]Present address: Department of Pharmacology, University of Michigan Medical School, Ann Arbor, MI 48109

NIH-PA Author Manuscript
NIH-PA Author Manuscript
NIH-PA Author Manuscript

NIH-PA Author Manuscript

NIH-PA Author Manuscript

NIH-PA Author Manuscript

lysophosphatidic acid, arachidonylglycerol-based endocannabinoids, and related lysolipids. S1P, which is widely distributed throughout the body, has been implicated in diverse physiological functions, including immune modulation, vascular and nervous system development, regulation of smooth muscle and auditory and vestibular function (Spiegel and Milstien 2003; Brinkmann 2007; Choi et al. 2008). S1P produces most of its physiological effects by binding to five G-protein coupled receptors, termed $S1P_{1-5}$ and formerly known as endothelial differential gene (EDG) receptors (Chun et al. 2002). At the cellular level, the balance between the actions of S1P and its precursors, ceramide and sphingosine, acts as a cellular rheostat that signals cell survival (S1P) or death (ceramide, sphingosine) (Spiegel and Milstien 2000). To date, the best defined therapeutic application of drugs targeting S1P receptors is the investigational immunomodulatory pro-drug FTY720 (fingolimod, 2-amino-2-(2-[4-octylphenyl]ethyl)-1,3-propanediol), a sphingosine analog that has shown promising results in clinical trials for treatment of multiple sclerosis (O'Connor et al. 2009).

S1P, its synthetic enzymes, sphingosine kinase 1 and 2, and S1P receptors are found in the CNS (Edsall and Spiegel 1999; Toman and Spiegel 2002; Blondeau et al. 2007; Bryan et al. 2008), where their role has been most clearly defined during neuronal development. In contrast, the putative function(s) of S1P in the adult CNS is only beginning to emerge. Recent studies suggest that S1P modulates neuronal excitability (Zhang et al. 2006; Kajimoto et al. 2007), but the mechanism underlying this action and its *in vivo* consequences are not well understood. S1P-stimulated G-protein activity has been reported, with activity widely distributed throughout the brain (Waeber and Chiu 1999). Localization of S1P receptor mRNA reveals that $S1P_1$, $S1P_2$ and $S1P_3$ receptors are widely distributed in the brain, with region-specific distributions and differential localization on neurons versus glia (Beer et al. 2000). In contrast, $S1P_5$ receptors are found primarily on oligodendrocytes and $S1P_4$ receptors are absent from the CNS (Terai et al. 2003; Brinkmann 2007). Despite increasing interest in S1P-mediated therapeutics and the identification of S1P receptors in the CNS, little is known regarding their role in neural function in the adult. Elucidation of S1P receptor-mediated CNS effects might have important implications for the development of novel therapeutics and could indicate potential CNS side effects of these drugs. The present study assessed S1P receptor function in the rodent CNS at both the cellular and *in vivo* levels. Because $S1P_1$ receptor-mediated G-protein activity appeared to predominate in several CNS regions, further studies concentrated on the role of $S1P_1$ receptors in CNS function. The results indicate that S1P receptors are part of a novel neuromodulatory system, and the anatomical distribution of S1P receptor-mediated G-protein activity and *in vivo* profile of S1P activity suggest that these receptors contribute to diverse CNS functions.

METHODS

Materials

S1P was purchased from Biomol and SEW2871was purchased from Cayman Chemical. VPC44116 was synthesized as described in Foss et al. (2007). SR141716A was provided by the National Institute on Drug Abuse Drug Supply Program. [^{35}S]GTPγS (1250 Ci/mmol) was purchased from Perkin Elmer. GDP was purchased from Sigma/RBI. All other reagent grade chemicals were obtained from Sigma or Fisher.

Agonist-stimulated [^{35}S]GTPγS autoradiography

Assays were conducted as previously described with slight modification (Sim et al. 1995). Mice were sacrificed by decapitation and brains were frozen in isopentane at -30°C. Twenty-micron coronal sections were cut on a cryostat at -20°C, thaw-mounted onto gelatin-coated slides and stored desiccated at -80°C. For assay, slides were brought to room temperature, then equilibrated in 50 mM Tris-HCl, pH 7.4, with 3 mM $MgCl_2$, 0.2 mM

NIH-PA Author Manuscript

NIH-PA Author Manuscript

NIH-PA Author Manuscript

EGTA, 100 mM NaCl (assay buffer) for 10 min at 25°C. Slides were transferred to assay buffer containing 0.5% bovine serum albumin (assay buffer + BSA) with 2 mM GDP and 9.5 mU/ml adenosine deaminase and incubated for 15 min at 25 °C. Slides were then incubated in assay buffer + BSA containing 2 mM GDP, 9.5 mU/ml adenosine deaminase and 0.04 nM [^{35}S]GTPγS in the presence or absence (basal) of appropriate concentrations of drugs/vehicle for 2 hours at 25°C. Concentration-effect curves were generated using 3 to 60 μM S1P and 3 to 80 μM SEW2871. Maximally effective concentrations of S1P (60 μM) or SEW2871 (80 μM) were calculated and used in the assay. Antagonist studies were conducted using EC_{75} concentrations of S1P (10 μM) or SEW (20 μM) with and without 50 μM VPC44116. After incubation, slides were rinsed twice in 50 mM Tris buffer (pH 7.4) at 4°C, then in deionized water. Slides were exposed to Biomax MR film with [^{14}C]microscales for 24 hours. Films were digitized and analyzed using NIH Image. Data are reported as mean values ± SEM of triplicate sections of brains from at least 7 mice per group. Net [^{35}S]GTPγS binding is defined as (agonist-stimulated [^{35}S]GTPγS binding - basal [^{35}S]GTPγS binding). [^{14}C] values were corrected for [^{35}S] based upon incorporation of [^{35}S] into sections of frozen brain paste. Statistical significance of the data was determined by ANOVA with appropriate post-hoc tests, as given in the figure legends.

Cortical cell cultures

Primary cultures of neurons plus glia were prepared using a modified version of Huettner and Baughman (1986). Neocortices were isolated from 1 to 2 day old Sprague-Dawley rats and digested using a 10 U/mL papain solution. Following trituration, cells were plated at a density of approximately 100-200 cells/mm^2 on a confluent layer of astrocytes in conditioned growth media consisting of MEM supplemented with 5% calf serum, 25 mM glucose, 100 U/mL penicillin, 100 ug/L streptomycin, and 500 nM glutamine. Cell cultures were incubated at 37°C an fed twice weekly with conditioned growth media. Cultures were utilized between 12-21 days in vitro (DIV).

Measurement of spontaneous excitatory postsynaptic currents (sEPSCs)

Using the whole-cell voltage clamp technique (Hamill et al. 1981), spontaneous excitatory postsynaptic currents were measured from individual cortical pyramidal neurons, identified by their characteristic morphology. Patch electrodes were made from borosilicate glass capillaries (WPI, Sarasota, FL) that were pulled to a tip resistance of 3-6 MΩ and filled with a solution containing (in mM): 135 K gluconate, 4 KCl, 2 NaCl, 10 EGTA, 0.2 $CaCl_2$, 2 MgATP, 0.6 Na_2GTP, 10 HEPES, pH 7.2. 285-295 mOsm The external recording solution contained (in mM): 130 NaCl, 4 KCl, 3 $CaCl_2$, 2 $MgCl_2$, 10 HEPES, 11 glucose, 0.01 glycine, and 0.05% BSA, pH 7.3, 295-305 mOsm. Solutions containing S1P, SEW2871, and VPC 44116 were made fresh daily from stock solutions of 10 mM drug in 5% 1N HCl:95% DMSO (vol:vol). All non-drug solutions contained 0.005% - 0.05% DMSO as a drug vehicle control. Drugs were applied using a SF-77 Perfusion Fast-Step system (Warner Ins. Co., Hamden, CT) as previously described (Goforth et al. 1999). Cells were continuously superfused with standard external solution at a rate of approximately 2 ml/min. Neurons used for analysis had stable series resistances (R_s) ≤30 MΩ and were compensated at ≥ 85%. All recordings were performed at room temperature.

Statistical analysis—sEPSC events were analyzed using Synaptosoft software (Decatur, GA). Individual events were detected using an amplitude threshold value of 4-6 pA and confirmed visually. Median sEPSC amplitude, 10-90% rise time, and half width were determined for each cell in the presence and absence of drug treatment and the mean median values of all cells were compared for each treatment. The total charge transfer resulting from sEPSC activity was calculated by integrating the current response over a 2 minute time period after baseline correction. Statistical analysis was performed using GraphPad Prism

NIH-PA Author Manuscript

NIH-PA Author Manuscript

NIH-PA Author Manuscript

2.0 (GraphPad Software Inc., San Diego, CA). Data are expressed as mean ± SEM. Data sets were tested for normality using the D'Agostino Pearson normality test. Significance was determined using ANOVA and Newman-Keuls multiple comparison post-hoc test (normal distributions) or Kruskal-Wallis and Dunn's post-hoc tests (non-parametric).

In vivo testing

Male ICR mice (Harlan Laboratories, Indianapolis, IN) weighing 25-30 g were housed in an animal facility maintained at 22 ± 2 °C on a 12-h light/dark cycle with *ad libitum* food and water. Mice were transported to the laboratory 6-8 h prior to testing to allow acclimation. All procedures were conducted in accordance with the regulations of the Institutional Animal Care and Use Committee at Virginia Commonwealth University and the Guide for the Care and Use of Laboratory Animals as promulgated by the National Institutes of Health. Six mice were tested per dose of drug or vehicle unless otherwise noted. S1P and SEW2871 were dissolved in acidified DMSO (5% 1N HCl:95% DMSO, vol:vol) and injected i.c.v. in a volume of 5μl/mouse (Pedigo et al. 1975). VPC44116 was prepared in acidified DMSO and administered i.c.v. 10 min prior to all drugs. SR141716A was dissolved in 1:1:18 (emulphor: ethanol: saline) and administered at a dose of 3 mg/kg, i.p. at 1 hr prior to i.c.v. administration of S1P, SEW2871 or vehicle. All drugs were freshly prepared before each use.

Antinociception—Baseline tail-flick latencies were determined prior to drug administration using the radiant heat tail-flick latency test (D'Amour and Smith 1941), and average values were between 2 and 4 sec. During testing, a cut-off time of 10 s was employed to prevent tail damage. Mice were not acclimated to the apparatus and were tested only twice - one baseline latency and one post-drug (test) latency. Antinociception was quantified using the percent maximal effect (%MPE) calculation (Harris and Pierson 1964): %MPE= [(test-baseline)/(maximum-baseline)] ×100 for each mouse. Mean % MPE ± SEM were recorded for each group of mice.

Rectal Temperature—Core temperature to the nearest 1°C was measured by inserting a rectal probe (2 cm into the rectum) connected to a Telethermometer. Baseline temperature was determined prior to drug administration. Following drug treatment, rectal temperature was measured at 1 min after test tail-flick latencies were determined, and values were expressed as the difference between control temperature (before injection) and temperatures following drug administration (°C).

Spontaneous Activity—After determination of tail-flick latency and rectal temperature, mice were placed in individual activity chambers, and spontaneous activity was measured for 10 min. Activity was measured as total number of interruptions of 16 photocell beams per chamber during the 10-min test and expressed as percentage inhibition of activity of the vehicle group.

Ring Immobility—Immediately after measurement of spontaneous activity, mice were placed on the ring immobility apparatus for 5 min (Pertwee 1972) and the total time (in seconds) that the mouse remained motionless was measured. The criterion for ring immobility was the absence of all voluntary movement, including snout and whisker movement. If a mouse fell or escaped from the ring apparatus during testing, it was immediately placed back on the ring. If it fell more than five times before 150 s had elapsed, data were omitted from analysis. The immobility is presented as the average of the total number of seconds that the mice remained immobile.

NIH-PA Author Manuscript

NIH-PA Author Manuscript

NIH-PA Author Manuscript

Data Analysis—Analysis of variance (ANOVA) was used to determine significant differences between control and treatment groups followed by Dunnett's or Newman-Keuls post hoc analysis. Statistical analysis was performed using Stat View, version 5.0 (SAS Institute, Cary, NC). Significance is defined as a $p < 0.05$. ED_{50} values were calculated by least squares linear regression analysis using at least 3 doses of drug, followed by calculation of 95% confidence limits according to the method of Bliss (1967).

RESULTS

S1P and SEW2871 stimulate [^{35}S]GTPγS binding in brain sections

The anatomical distribution of S1P-stimulated [^{35}S]GTPγS autoradiography was determined and compared to that produced by the $S1P_1$ receptor-selective agonist SEW2871. Visual inspection revealed that S1P and SEW2871 stimulated [^{35}S]GTPγS binding throughout the brain, with levels of activity varying by region (Fig. 1a), as confirmed by quantitative densitometry (Fig. 1b). The highest levels of S1P-stimulated activity were seen throughout the cortex, molecular layer of the cerebellum (Cblm) and amygdala (Amyg) (Fig. 1a, b). SEW2871-stimulated activity was also highest in these regions and comprised approximately 65-75% of total S1P-stimulated activity (Fig 1c). Moderate levels of S1P-stimulated activity were found in the caudate-putamen (CPu), periaqueductal gray (PAG), hippocampus (Hip) and hypothalamus (Hyp) (Fig. 1a, b). SEW2871 also stimulated [^{35}S]GTPγS binding in these regions and appeared to represent approximately 40% of total S1P-stimulated activity (Fig. 1c). Lower levels of S1P-stimulated [^{35}S]GTPγS binding were detected in thalamus (Thal) and corpus callosum (cc) (Fig. 1a, b) and $S1P_1$ receptors appeared to contribute only minimally to activity in these regions, as indicated by SEW2871 (Fig. 1b, c).

S1P- and SEW2871-stimulated [^{35}S]GTPγS binding are inhibited by the $S1P_{1/3}$ receptor antagonist VPC44116

The contribution of $S1P_1$ receptors to total S1P-stimulated [^{35}S]GTPγS binding was further assessed by incubating the $S1P_{1/3}$ antagonist VPC44116 with EC_{75} concentrations of S1P and SEW2871. VPC44116 is a competitive antagonist at $S1P_1$ receptors with a K_i value of 25 nM, whereas it is approximately 10-fold less potent at $S1P_3$ receptors (Foss et al. 2007). VPC44116 is also a partial agonist of $S1P_4$ and $S1P_5$ receptors, although it has very low (>6 μM) affinity for $S1P_4$, and does not have significant affinity for $S1P_2$ (Foss et al. 2007). As seen in cerebellum (Fig. 2a) and cingulate cortex (Fig. 2b), incubation with VPC44116 alone did not significantly alter [^{35}S]GTPγS binding, but incubation of VPC44116 with either S1P or SEW2871 completely blocked agonist-stimulated G-protein activity. Similar results were obtained in most other regions examined (data not shown), including amygdala, PAG, and hypothalamus, where both S1P and SEW2871 produced significant stimulation that was completely blocked by incubation with VPC44116 ($p < 0.001$ by Newman-Keuls test). Interestingly, S1P at this lower concentration produced only minimal stimulation of [^{35}S]GTPγS binding in regions including caudate-putamen, corpus callosum and thalamus, suggesting possible regional differences in the potency of S1P to activate G-proteins (data not shown).

S1P suppresses excitatory synaptic transmission

Exogenous S1P induces glutamate release in primary hippocampal neurons (Kajimoto et al. 2007). To determine whether the activation of S1P receptors and concomitant G-protein activity affects neurotransmission, we examined the effect of S1P receptor agonists on excitatory synaptic transmission between cortical neurons *in vitro*. Spontaneous excitatory postsynaptic currents (or sEPSCs) of individual cortical pyramidal neurons were isolated from GABAergic inhibitory postsynaptic currents (IPSCs), by voltage- clamping neurons to

NIH-PA Author Manuscript

NIH-PA Author Manuscript

NIH-PA Author Manuscript

the reversal potential of the IPSCs (~ -65 mV). All remaining events were glutamatergic because they were blocked by the glutamate receptor antagonists CNQX (10 μM) and APV (20 μM; data not shown). Cultured cortical neurons exhibited spontaneous excitatory synaptic currents (Fig. 3) and 1 μM S1P reduced sEPSC frequency and amplitude. Thus, S1P significantly reduced mean sEPSC frequency by 27.3 ± 9.5% (n=11, p< 0.04, Fig. 3b) and mean median sEPSC amplitude by 12.7 ± 2.7% (n=10, p < 0.01, Fig. 3c). S1P had no significant effect on sEPSC rise time (10-90%) or half width (data not shown). The combined decrease in sEPSC frequency and amplitude resulted in significant reduction of the total charge transfer during excitatory synaptic transmission, as mean charge transfer in the presence of 1 μM S1P decreased by 42.0 ± 5.3% (n=10, p < 0.001, Fig. 3d). Thus, S1P appears to suppress overall excitatory input, with changes in sEPSC frequency most likely resulting from diminished presynaptic glutamate release.

S1P-induced alterations of sEPSCs are mediated by $S1P_1$ receptors

The $S1P_{1/3}$ antagonist, VPC44116 was used to determine whether S1P modulation of sEPSCS required $S1P_{1/3}$ receptor activation. VPC44116 partially reversed the effects of S1P on sEPSC amplitude, frequency, and charge transfer (Fig. 4). As previously demonstrated, 1 μM S1P significantly reduced mean sEPSC frequency by 57.1 ± 16.7% (n=5, p< 0.03 vs. control, Fig. 4a) while the subsequent co- application of 1 μM S1P + 5 μM VPC44116 returned sEPSC frequency to 69.0 ± 21.6% of control (n=5, p > 0.05 vs. control). Of note, sEPSC frequency varied between individual cells and cell preparations even without drug treatment, and the degree to which S1P reduced sEPSC frequency was also heterogeneous. This may reflect, in part, differing degrees of endogenous S1P activity, which we did not independently determine. Mean median sEPSC amplitude, while not significant in this data set, exhibited a similar trend and decreased to 75.0 ± 7.5% of control amplitude in the presence of 1 μM S1P only (n=5, p > 0.05 vs. control), but returned to 96.7 ± 15.8% of control amplitude following the addition of 5 μM VPC44116 (Fig. 4c). VPC44116 also reversed the reduction in overall charge transfer induced by S1P (Fig. 4d), whereby S1P decreased mean charge transfer by 54.4 ± 9.1% (n=5, p < 0.002 vs. control), and the subsequent addition of VPC44116 restored charge transfer to 87.3 ± 9.4% of control (n=5, p > 0.05 vs. control; p < 0.01 vs. 1 μM S1P only). The ability of VPC44116 to reverse S1P modulation of sEPSCs suggests that S1P modulation is mediated, at least in part, by the activation of $S1P_1$ receptors. A similar suppression of sEPSC activity was observed using the selective $S1P_1$ receptor agonist SEW2871 (Fig. 5). In 8/9 neurons, SEW2871 (20 μM) reduced sEPSC charge transfer by 43.8 ± 8.2% (n=8, p < 0.05), and the addition of VPC44116 in the continued presence of SEW2871 restored charge transfer to 85.5 ± 10.1% of control. The localization of $S1P_1$ receptors in cortical cultures was confirmed by immunofluorescence with confocal microscopy (supplemental data). $S1P_1$ receptor immunoreactivity was found in cortical pyramidal neurons, most of which appeared to be glutamatergic, as indicated by the presence of immunoreactivity for the vesicular glutamate transporter. These results extend those obtained using agonist-stimulated [^{35}S]GTPγS autoradiography to show that S1P functionally modifies synaptic transmission in the cortex acutely.

S1P produces antinociception to thermal stimulus via $S1P_1$ receptors

Because S1P produced changes in both receptor-mediated G-protein activity and functional synaptic transmission, it was next determined whether S1P-mediated changes could produce *in vivo* effects. The effect of S1P on thermal nociception in mice using the tail withdrawal was selected because it is a reflex and would not be confounded by possible effects on motor activity or core body temperature (Lichtman et al. 1993). Dose-response curves were generated for S1P-mediated antinociception using the tail flick assay after i.c.v. injection of S1P (Fig. 6a). Time-course studies determined that the peak time of antinociceptive activity

NIH-PA Author Manuscript

NIH-PA Author Manuscript

NIH-PA Author Manuscript

was 15-20 minutes and the offset of antinociceptive activity occurred within 30 minutes (data not shown). S1P elicited dose-dependent antinociception, with an ED_{50} value of 19.1 μg [17.6-20.8]. Due to solubility limitations, doses higher than 25 μg/mouse i.c.v. were not tested. Thermal antinociception was also observed with the $S1P_1$-selective agonist, SEW2871. The peak effect in the tail flick test was 45.7 ± 21.6 %MPE, observed 10 minutes after the i.c.v. administration of 50 μg SEW2871. However, solubility of the drug was poor at concentrations needed to test higher doses, so no ED_{50} value could be calculated. In all studies, the vehicle control (acidified DMSO) was administered i.c.v. and produced 18 ± 5 %MPE.

To further examine the contribution of specific S1P receptor types to in vivo activity, the effect of the $S1P_{1/3}$-selective antagonist VPC44116 was also assessed in the tail-flick assay (Fig. 6b). Administration of vehicle or VPC44116 alone (25 μg i.c.v.) had no significant effect on tail withdrawal latency (10 ± 4 %MPE, 24 ± 5 %MPE, respectively). S1P (25 μg i.c.v.) and SEW2871 (50 μg i.c.v.) were administered and the tail-flick assay was conducted 10 (SEW2871) or 15 (S1P) minutes following injection. Under these conditions, S1P produced 87 ± 7 %MPE whereas SEW2871 produced 40 ± 28 %MPE. For antagonist studies, VPC44116 (25 μg i.c.v.) was administered 10 (S1P) or 15 (SEW) minutes prior to agonist and mice were tested at 25 minutes post-VPC44116 injection. In both cases, pretreatment with VPC44116 significantly inhibited antinociception produced by the agonist ($p < 0.01$) [12.6 ± 2 %MPE, 4 ± 2 %MPE, respectively, for S1P and SEW2871]. These results provide further evidence that S1P produces thermal antinociception via an $S1P_1$ receptor-mediated mechanism.

S1P produces hypoactivity, catalepsy, hypothermia and antinociception

Studies were next conducted to determine whether there were additional *in vivo* effects of centrally administered S1P. Because of the homology between S1P and cannabinoid receptors (Toman and Spiegel 2002), their similar anatomical distributions in the CNS (Herkenham et al. 1991; present study) and the ability of both cannabinoids and S1P to mediate thermal antinociception, a tetrad of *in vivo* measures that are characteristic of the CNS-mediated effects of cannabinoids was assessed (Compton et al. 1993). Mice were injected with S1P (25 μg i.c.v.) and tested as described in Methods. Antinociception was determined at 15 minutes post-administration of S1P followed immediately by the determination of rectal temperature, spontaneous activity (assessed by beam breaks) and catalepsy (ring immobility). As expected, a significant antinociceptive effect of S1P was again observed (Fig. 7a). Interestingly, mice that received S1P also exhibited significant hypothermia (Fig. 7b), catalepsy (Fig. 7c) and inhibition of locomotor activity (Fig. 7d).

To determine whether these effects of S1P were $S1P_{1/3}$ receptor mediated, the $S1P_{1/3}$ antagonist, VPC44116, or vehicle were administered 10 minutes prior to administration of S1P or vehicle, and mice were then tested as described above. Surprisingly, the administration of VPC44116 alone produced significant hypothermia, catalepsy and decreased spontaneous activity when compared to vehicle administration (Fig. 7, b-d). In contrast, VPC44116 alone did not produce antinociception, but significantly blocked the antinociceptive effects of S1P (Fig. 7a), similar to the results presented above. VPC44116 did not enhance the hypothermia, catalepsy or hypoactivity produced by S1P, and in fact appeared to produce partial reversal of S1P-induced catalepsy (Fig. 7d).

Because the tetrad of effects described above is reliably produced by cannabinoids, these tests were repeated with S1P in the presence and absence of the CB_1-selective antagonist rimonabant (SR141716A). Moreover, because certain sphingosine derivatives can act as CB_1 antagonists (Paugh et al. 2006), it was important to determine if there is any involvement of the cannabinoid system in mediation of these effects. As observed above,

NIH-PA Author Manuscript

NIH-PA Author Manuscript

NIH-PA Author Manuscript

S1P produced antinociception (Fig. 8a) and hypothermia (Fig. 8b). Administration of the CB_1 antagonist rimonabant (3mg/kg) did not significantly block these S1P-mediated effects, nor did the cannabinoid antagonist have significant intrinsic effects in any of the tests at the doses administered (Fig. 8a, b). Similar results were obtained with hypomotility and catalepsy (data not shown). These results demonstrate that while S1P produced cannabinoid-like *in vivo* effects, these actions were independent of CB_1 receptors. However, due to the apparent intrinsic effects of VPC44116 on body temperature and motor activity, only antinociception could be definitively attributed to the activation of $S1P_{1/3}$ receptors.

DISCUSSION

The current study revealed that S1P activated G-proteins in anatomically distinct brain regions and reduced excitatory neuronal activity in cortical neurons, presumably by reducing synaptically released glutamate, consistent with the hypothesis that S1P is a functionally active neuromodulator. The effect of S1P on agonist-stimulated [^{35}S]GTPγS binding appeared to result largely from activity at $S1P_1$ receptors in certain regions of the brain, including cortex, cerebellum and amygdala. Additionally, *in vivo* administration of S1P produced antinociception, hypoactivity, catalepsy and hypothermia, although only antinociception could be definitively attributed to $S1P_1$ receptors, as indicated by the antinociceptive action of the $S1P_1$-selective agonist SEW2871 and reversibility by the $S1P_{1/3}$-selective antagonist VPC44116. To our knowledge, this is the first study to elucidate the role of a specific S1P receptor type in CNS-mediated effects in adult animals, and the results suggest that $S1P_1$ receptors play an important functional role in the adult brain. This finding is particularly significant because the immunomodulatory agent FTY720 produces reversible lymphopenia via activity at $S1P_1$ receptors (Mandala et al. 2002) and shows promise for treatment of multiple sclerosis (O'Connor et al. 2009) and possibly other autoimmune disorders (Brinkmann 2007). Thus, $S1P_1$ receptors are an emerging therapeutic target and the results of this study suggest additional applications, for example as analgesics or modulators of glutamatergic neurotransmission. Additionally, the possibility that drugs acting at S1P receptors will produce CNS side effects, such as motor impairment or hypothermia, should be considered. Alternatively, S1P might also produce intracellular effects independently of its action at S1P receptors in the CNS, as previously observed in some non-neural cell types (Spiegel and Milstien 2000).

The current studies utilized $S1P_1$-selective ligands to assess the role of this receptor in CNS function. In contrast, compounds selective for $S1P_2$, $S1P_3$ and $S1P_5$ receptors have proven to be more challenging to develop (Lynch and Macdonald 2008). Although $S1P_1$ receptors are clearly involved in CNS function, the current results suggest that other S1P receptor types might also be involved. Most notably, measures of hypomotility, hypothermia and catalepsy induced by S1P were confounded by the intrinsic *in vivo* effects of VPC44116. Moreover, $S1P_1$ receptor-mediated G-protein activity stimulated by S1P was not fully mimicked by SEW2871. In fact, the contribution of $S1P_1$ receptors to total G-protein activity based on a comparison between S1P and SEW2871 varied from approximately 10% in thalamus and corpus callosum to approximately 75% in cortex and cerebellum. It is also possible that the relative contribution of $S1P_1$ receptors attributed to SEW2871 could have been underestimated if this ligand acted as a partial agonist relative to S1P. However, SEW2871 appeared to be a full agonist for stimulation of [^{35}S]GTPγS binding in CHO cells stably expressing $S1P_1$ receptors (Sanna et al. 2004). Nonetheless, it should be noted that the relative efficacy of GPCR partial agonists could appear to be greater in transfected cell preparations than brain membranes due to differences in receptor reserve (Selley et al. 1998). This concept might also explain why Sanna et al. observed a >15-fold greater EC_{50} value of SEW2871 relative to S1P, whereas preliminary concentration-effect curves for

NIH-PA Author Manuscript

NIH-PA Author Manuscript

NIH-PA Author Manuscript

stimulation of [^{35}S]GTPγS binding to cerebellar sections indicated only 1.5-fold difference in the potency of these two drugs (data not shown).

Because selective ligands are lacking for most of the S1P receptor types, information on the localization of specific S1P receptors has been inferred from in situ hybridization studies (Beer et al. 2000). $S1P_1$ receptor mRNA was highest in cerebellum, and $S1P_3$ receptor mRNA, while only weakly expressed, was highest in the cortex. $S1P_2$ receptor mRNA was most abundant among hippocampal neurons. In contrast, $S1P_5$ receptor mRNA is reportedly confined to oligodendrocytes (Terai et al. 2003). The present findings, combined with the CNS distribution of mRNA for other S1P receptor types, suggest that $S1P_3$ and possibly $S1P_2$ receptors might also contribute to neural function. Similarly, S1P receptor types exhibit distinct signaling profiles (Takabe et al. 2008). All of the S1P receptors activate $G_{i/o}$ and all except $S1P_1$ receptors couple to $G_{12/13}$. In addition, $S1P_2$ and $S1P_3$ receptors couple to $G_{q/11}$, suggesting that activation of these receptors might produce different intracellular effects compared to $S1P_1$ receptors.

The generation of mice lacking specific S1P receptors has provided further insights into the role of the different S1P receptor types, but few studies have directly examined effects in the CNS (Choi et al. 2008). $S1P_1$ receptor deletion is lethal due to inadequate vascular maturation and resulting embryonic hemorrhage (Liu et al. 2000). $S1P_3$ receptor null mice have significantly reduced litters, suggesting reproductive/developmental deficits, and alterations in receptor signaling (Ishii et al. 2001), but do not exhibit a marked phenotype. $S1P_2$ receptor deficient mice have auditory and vestibular deficits due to cochlear hair cell loss and vascular disturbances (Brinkmann 2007; Choi et al. 2008). Deletion of $S1P_2$ receptors also increased seizure activity due to hyperexcitability of cortical pyramidal neurons (MacLennan et al. 2001), but not all $S1P_2$ null lines exhibit this phenotype.

The results observed in cortical neurons are consistent with the possibility that certain S1P receptors negatively regulate neuronal activity. In the present study, $S1P_1$ receptors were found to inhibit synaptic glutamate release in cortical neurons, as indicated by the effectiveness of the $S1P_1$ agonist SEW2871 and reversal by the $S1P_{1/3}$ antagonist VPC44116. While these data appear to contradict a recent report of S1P-induced stimulation of glutamate secretion in hippocampal neurons (Kajimoto et al. 2007), the measurement of EPSCs provides a more direct assay of synaptic glutamatergic function and raises the possibility that the previously observed increase in overall extracellular glutamate might not be localized synaptically (Kajimoto et al. 2007). It is also possible that S1P-mediated effects on neuronal activity are region and receptor dependent. Thus, S1P-stimulated glutamate release in primary cultures of hippocampal neurons was attributed to both $S1P_1$ and $S1P_3$ receptors, based on PCR analysis and inhibition of the effects by siRNA knockdown (Kajimoto et al. 2007). S1P was also reported to increase excitability of small diameter sensory neurons isolated from dorsal root ganglia via GPCR-mediated effects on Na^+ and K^+ channels (Zhang et al. 2006). These authors suggested that S1P might therefore contribute to the hypersensitivity observed during inflammation. Indeed, FTY720 was recently reported to reduce antinociception in the formalin assay, a model of inflammation (Coste et al. 2008), but interpretation is complicated by the fact that FTY720 can inhibit cPLA2 (Payne et al. 2007) and thus prostaglandins, whereas FTY720-P is an agonist at four of the S1P receptors. Nevertheless, considered in light of the present finding that S1P produces antinociception to thermal stimuli, the S1P system is emerging as a novel analgesic target.

In summary, this report demonstrates that S1P receptors are part of a novel neuromodulatory system in the CNS and that administration of S1P agonist regulates nociception, body temperature and motor activity. Moreover, the application of $S1P_1$ selective ligands in both

NIH-PA Author Manuscript

NIH-PA Author Manuscript

NIH-PA Author Manuscript

cellular and *in vitro* assays revealed that $S1P_1$ receptors produce high levels of G-protein activity throughout multiple brain regions and regulate neuronal excitability via the inhibition of glutamatergic transmission in the cortex. Additionally, $S1P_1$ receptors mediate antinociception to thermal stimuli. The data further reveal that activation of other types of S1P receptors might produce G-protein activity and might contribute to S1P-mediated modulation of hypothermia, motor function and catalepsy, although these behavioral effects could be mediated in part via non-receptor effects of S1P. These studies support the concept that S1P and S1P receptors in the brain are important regulators of CNS function and should be considered both for novel therapeutic targets and potential side effects.

Supplementary Material

Refer to Web version on PubMed Central for supplementary material.

Acknowledgments

These studies were supported by USPHS grants R01 DA014277 (LJS), R01 DA10770 (DES), R03 DA022581 (SPW), R01 GM043880 (SS), R01 NS049519 (LSS), R01 GM067958 (KRL & TLM), the Thomas F. and Kate Miller Jeffress Memorial Trust (LJS, SPW) and the NIMH Intramural Research Program (SM). The authors thank Dr. Katherine Falenski, James Burston, Peter Nguyen and David Stevens for assistance.

REFERENCES

Beer MS, Stanton JA, Salim K, Rigby M, Heavens RP, Smith D, McAllister G. EDG receptors as a therapeutic target in the nervous system. Ann. N. Y. Acad. Sci. 2000; 905:118–131. [PubMed: 10818448]

Bliss, CI. Statistics in Biology. McGraw-Hill; New York: 1967.

Blondeau N, Lai Y, Tyndall S, Popolo M, Topalkara K, Pru JK, Zhang L, Kim H, Liao JK, Ding K, Waeber C. Distribution of sphingosine kinase activity and mRNA in rodent brain. J. Neurochem. 2007; 103:509–517. [PubMed: 17623044]

Brinkmann V. Sphingosine 1-phosphate receptors in health and disease: Mechanistic insights from gene deletion studies and reverse pharmacology. Pharmacol. Ther. 2007; 115:84–105. [PubMed: 17561264]

Bryan L, Kordula T, Spiegel S, Milstien S. Regulation and functions of sphingosine kinases in the brain. Biochim. Biophys. Acta. 2008

Choi JW, Lee CW, Chun J. Biological roles of lysophospholipid receptors revealed by genetic null mice: An update. Biochim. Biophys. Acta. 2008

Chun J, Goetzl EJ, Hla T, Igarashi Y, Lynch KR, Moolenaar W, Pyne S, Tigyi G. International Union of Pharmacology. XXXIV. Lysophospholipid receptor nomenclature. Pharmacol. Rev. 2002; 54:265–269. [PubMed: 12037142]

Compton DR, Rice KC, DeCosta BR, Razdan RK, Melvin LS, Johnson MR, Martin BR. Cannabinoid structure-activity relationships: Correlation of receptor binding and *in vivo* activities. J. Pharmacol. Exp. Ther. 1993; 265:218–226. [PubMed: 8474008]

Coste O, Pierre S, Marian C, Brenneis C, Angioni C, Schmidt H, Popp L, Geisslinger G, Scholich K. Antinociceptive activity of the S1P-receptor agonist FTY720. J Cell Mol Med. 2008; 12:995–1004. [PubMed: 18494940]

D'Amour FE, Smith DC. A method for determining the loss of pain sensation. J. Pharmacol. Exp. Ther. 1941; 72:74–79.

Edsall LC, Spiegel S. Enzymatic measurement of sphingosine 1-phosphate. Anal. Biochem. 1999; 272:80–86. [PubMed: 10405296]

Foss FW Jr. Snyder AH, Davis MD, Rouse M, Okusa MD, Lynch KR, Macdonald TL. Synthesis and biological evaluation of gamma-aminophosphonates as potent, subtype-selective sphingosine 1-phosphate receptor agonists and antagonists. Bioorg. Med. Chem. 2007; 15:663–677. [PubMed: 17113298]

NIH-PA Author Manuscript

NIH-PA Author Manuscript

NIH-PA Author Manuscript

Goforth PB, Ellis EF, Satin LS. Enhancement of AMPA-mediated current after traumatic injury in cortical neurons. J. Neurosci. 1999; 19:7367–7374. [PubMed: 10460243]

Hamill OP, Marty A, Neher E, Sakmann B, Sigworth FJ. Improved patch-clamp techniques for high-resolution current recording from cells and cell-free membrane patches. Pflugers Arch. 1981; 391:85–100. [PubMed: 6270629]

Harris LS, Pierson AK. Some Narcotic Antagonists In The Benzomorphan Series. J. Pharmacol. Exp. Ther. 1964; 143:141–148. [PubMed: 14163985]

Herkenham M, Lynn AB, Johnson MR, Melvin LS, de Costa BR, Rice KC. Characterization and localization of cannabinoid receptors in rat brain: a quantitative in vitro autoradiographic study. J. Neurosci. 1991; 11:563–583. [PubMed: 1992016]

Huettner JE, Baughman RW. Primary culture of identified neurons from the visual cortex of postnatal rats. J. Neurosci. 1986; 6:3044–3060. [PubMed: 3760948]

Ishii I, Friedman B, Ye X, Kawamura S, McGiffert C, Contos JJ, Kingsbury MA, Zhang G, Brown JH, Chun J. Selective loss of sphingosine 1-phosphate signaling with no obvious phenotypic abnormality in mice lacking its G protein-coupled receptor, LP(B3)/EDG-3. J. Biol. Chem. 2001; 276:33697–33704. [PubMed: 11443127]

Kajimoto T, Okada T, Yu H, Goparaju SK, Jahangeer S, Nakamura S. Involvement of sphingosine-1-phosphate in glutamate secretion in hippocampal neurons. Mol. Cell. Biol. 2007; 27:3429–3440. [PubMed: 17325039]

Lichtman AH, Smith FL, Martin BR. Evidence that the antinociceptive tail-flick response is produced independently from changes in either tail-skin temperature or core temperature. Pain. 1993; 55:283–295. [PubMed: 8121689]

Liu Y, Wada R, Yamashita T, Mi Y, Deng CX, Hobson JP, Rosenfeldt HM, Nava VE, Chae SS, Lee MJ, Liu CH, Hla T, Spiegel S, Proia RL. Edg-1, the G protein-coupled receptor for sphingosine-1-phosphate, is essential for vascular maturation. J. Clin. Invest. 2000; 106:951–961. [PubMed: 11032855]

Lynch KR, Macdonald TL. Sphingosine 1-phosphate chemical biology. Biochim. Biophys. Acta. 2008; 1781:508–512. [PubMed: 18638568]

MacLennan AJ, Carney PR, Zhu WJ, Chaves AH, Garcia J, Grimes JR, Anderson KJ, Roper SN, Lee N. An essential role for the H218/AGR16/Edg-5/LP(B2) sphingosine 1-phosphate receptor in neuronal excitability. Eur. J. Neurosci. 2001; 14:203–209. [PubMed: 11553273]

Mandala S, Hajdu R, Bergstrom J, Quackenbush E, Xie J, Milligan J, Thornton R, Shei GJ, Card D, Keohane C, Rosenbach M, Hale J, Lynch CL, Rupprecht K, Parsons W, Rosen H. Alteration of lymphocyte trafficking by sphingosine-1-phosphate receptor agonists. Science. 2002; 296:346–349. [PubMed: 11923495]

O'Connor P, Comi G, Montalban X, Antel J, Radue EW, de Vera A, Pohlmann H, Kappos L. Oral fingolimod (FTY720) in multiple sclerosis: two-year results of a phase II extension study. Neurology. 2009; 72:73–79. [PubMed: 19122034]

Paugh SW, Cassidy MP, He H, Milstien S, Sim-Selley LJ, Spiegel S, Selley DE. Sphingosine and its analog, the immunosuppressant 2-amino-2-(2-[4- octylphenyl]ethyl)-1,3-propanediol, interact with the CB1 cannabinoid receptor. Mol. Pharmacol. 2006; 70:41–50. [PubMed: 16571654]

Payne SG, Oskeritzian CA, Griffiths R, Subramanian P, Barbour SE, Chalfant CE, Milstien S, Spiegel S. The immunosuppressant drug FTY720 inhibits cytosolic phospholipase A2 independently of sphingosine-1-phosphate receptors. Blood. 2007; 109:1077–1085. [PubMed: 17008548]

Pedigo NW, Dewey WL, Harris LS. Determination and characterization of the antinociceptive activity of intraventricularly administered acetylcholine in mice. J. Pharmacol. Exp. Ther. 1975; 193:845–852. [PubMed: 1151733]

Pertwee RG. The ring test: a quantitative method for assessing the `cataleptic' effect of cannabis in mice. Br. J. Pharmacol. 1972; 46:753–763. [PubMed: 4655271]

Sanna MG, Liao J, Jo E, Alfonso C, Ahn MY, Peterson MS, Webb B, Lefebvre S, Chun J, Gray N, Rosen H. Sphingosine 1-phosphate (S1P) receptor subtypes S1P1 and S1P3, respectively, regulate lymphocyte recirculation and heart rate. J. Biol. Chem. 2004; 279:13839–13848. [PubMed: 14732717]

NIH-PA Author Manuscript

NIH-PA Author Manuscript

NIH-PA Author Manuscript

Selley DE, Liu Q, Childers SR. Signal transduction correlates of mu opioid agonist intrinsic efficacy: receptor-stimulated [^{35}S]GTP gamma S binding in mMOR-CHO cells and rat thalamus. J. Pharmacol. Exp. Ther. 1998; 285:496–505. [PubMed: 9580589]

Sim, LJ.; Selley, DE.; Childers, SR. *In vitro* autoradiography of receptor-activated G-proteins in rat brain by agonist-stimulated guanylyl 5'-[γ-[^{35}S]thio]-triphosphate binding. Proceedings of the National Academy of Sciences USA; 1995. p. 7242-7246.

Spiegel S, Milstien S. Sphingosine-1-phosphate: signaling inside and out. FEBS Lett. 2000; 476:55–57. [PubMed: 10878250]

Spiegel S, Milstien S. Sphingosine-1-phosphate: an enigmatic signalling lipid. Nat Rev Mol Cell Biol. 2003; 4:397–407. [PubMed: 12728273]

Takabe K, Paugh SW, Milstien S, Spiegel S. "Inside-out" signaling of sphingosine-1-phosphate: therapeutic targets. Pharmacol. Rev. 2008; 60:181–195. [PubMed: 18552276]

Terai K, Soga T, Takahashi M, Kamohara M, Ohno K, Yatsugi S, Okada M, Yamaguchi T. Edg-8 receptors are preferentially expressed in oligodendrocyte lineage cells of the rat CNS. Neuroscience. 2003; 116:1053–1062. [PubMed: 12617946]

Toman RE, Spiegel S. Lysophospholipid receptors in the nervous system. Neurochem. Res. 2002; 27:619–627. [PubMed: 12374197]

Waeber C, Chiu ML. In vitro autoradiographic visualization of guanosine-5'-*O*-(3-[^{35}S]thio)triphosphate binding stimulated by sphingosine 1-phosphate and lysophosphatidic acid. J. Neurochem. 1999; 73:1212–1221. [PubMed: 10461914]

Zhang YH, Fehrenbacher JC, Vasko MR, Nicol GD. Sphingosine-1-phosphate via excitation of a G-protein-coupled receptor(s) enhances the excitability of rat sensory neurons. J. Neurophysiol. 2006; 96:1042–1052. [PubMed: 16723416]

NIH-PA Author Manuscript
NIH-PA Author Manuscript
NIH-PA Author Manuscript

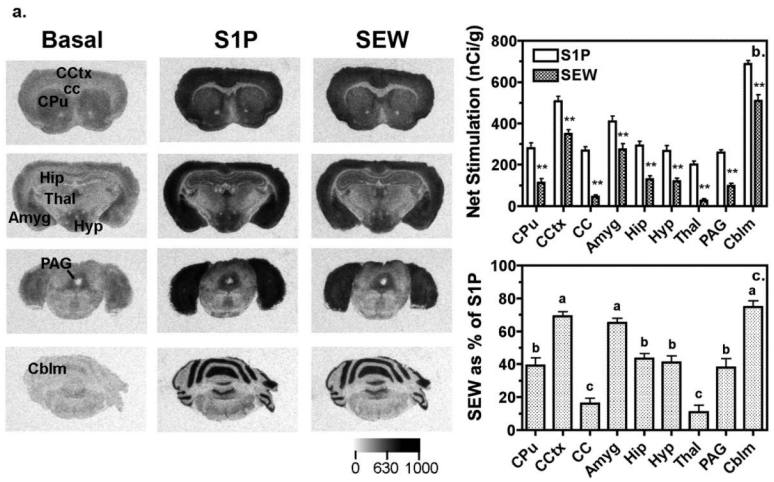

Figure 1.

Representative autoradiograms and densitometric analysis reveal region-specific S1P-and SEW2871-stimulated G-protein activity in mouse brain. **a**.) Autoradiograms show basal binding in the absence of agonist (left column) and stimulation of [^{35}S]GTPγS binding by 60 μM S1P (center column) or 80 μM SEW2871 ($S1P_1$-selective agonist, right column). **b**.) Densitometric analysis of S1P-and SEW2871-stimulated [^{35}S]GTPγS binding in the brain reveal regional differences in the magnitude of G-protein activation. Data are expressed as net agonist-stimulated activity ± SEM. **, SEW2871 was $p < 0.01$ different from S1P by 2-way ANOVA (drug x region) with post-hoc Bonferroni test (n = 10-12). **c**.) SEW2871-stimulated [^{35}S]GTPγS binding, expressed as a percent of S1P-stimulated activity in the brain, varies among brain regions, suggesting that $S1P_1$ receptors contribute varying proportions of the total G-protein activation seen with S1P in different brain regions. Regions with different letter designations are $p < 0.05$ different from each other by ANOVA with post-hoc Newman-Keuls test (n = 10-12). Abbreviations: Amyg; amygdala, Cblm; cerebellum, cc; corpus callosum, CCtx; cingulated cortex, CPu; caudate-putamen, Hip; hippocampus, Hyp; hypothalamus, PAG; periaqueductal gray, Thal; thalamus.

NIH-PA Author Manuscript
NIH-PA Author Manuscript
NIH-PA Author Manuscript

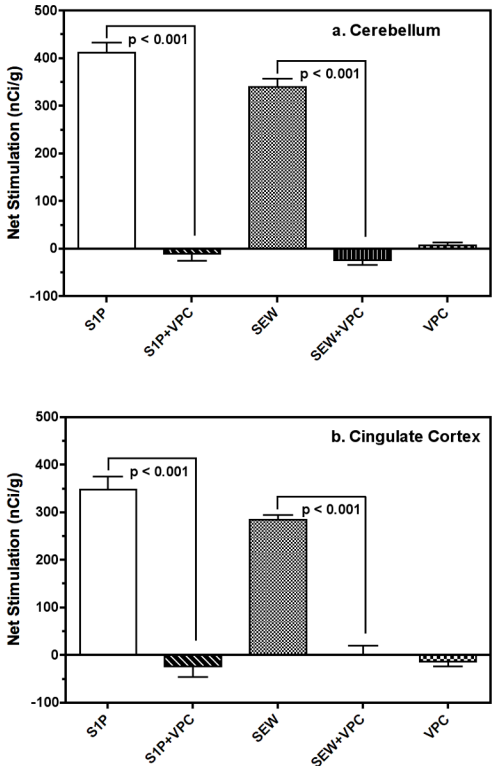

Figure 2.

Net S1P- and SEW2871-stimulated G-protein activity in cerebellum and cingulate cortex is inhibited by the $S1P_{1/3}$ antagonist VPC44116. Sections at the level of the **a**.) cerebellum or **b**.) cingulate cortex were incubated with vehicle (basal), S1P (10 μM) or SEW2871 (20 μM) in the presence and absence of the $S1P_{1/3}$ antagonist VPC44116 (50 μM). VPC44116 blocked the stimulation of [^{35}S]GTPγS binding by S1P or SEW2871, but did not affect [^{35}S]GTPγS binding by itself. [^{35}S]GTPγS binding is expressed as mean net stimulate [^{35}S]GTPγS binding ± SEM. The p values shown were obtained by ANOVA with post-hoc Newman-Keuls test (n = 6-7).

NIH-PA Author Manuscript

NIH-PA Author Manuscript

NIH-PA Author Manuscript

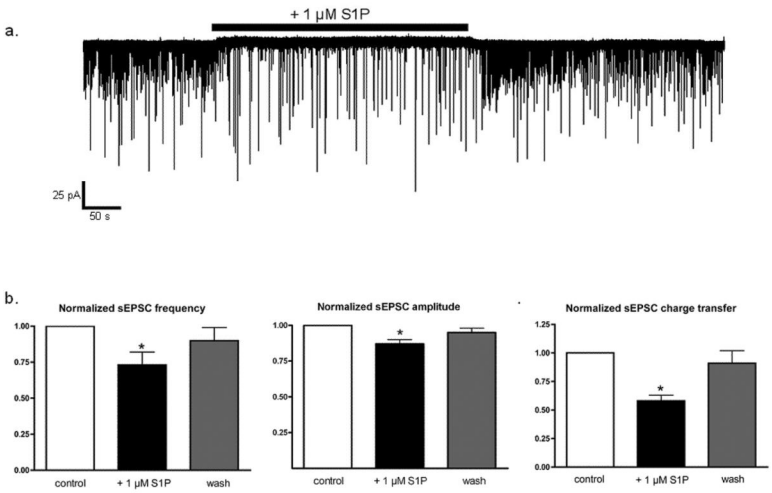

Figure 3.

S1P decreases sEPSC frequency and amplitude in cortical pyramidal neurons. **a**.) Whole-cell recording of sEPSCs (downward deflections) from an individual cortical pyramidal neuron. Application of 1 μM S1P (black bar) reduced sEPSC frequency and amplitude. **b**.) sEPSC parameters for each condition were normalized to the pre-drug value in each neuron. 1 μM S1P decreased mean sEPSC frequency by 27.3 ± 9.5% (n=11, $p < 0.04$ vs. control, ANOVA) and sEPSC frequency returned to 90.1 ± 9.5% of control frequency after removal of S1P. **c**.) 1 μM S1P decreased mean sEPSC amplitude by 12.7 ± 2.7% (n=10, $p < 0.01$ vs. control) and sEPSC amplitude returned to 94.7 ± 2.6% of control values after wash. **d**.) 1 μM S1P decreased mean sEPSC charge transfer by 42.0 ± 5.3% (n=10, $p < 0.001$ vs. control) and sEPSC charge transfer returned to 90.8 ± 10.8% of control values after wash. Statistical significance was determined by ANOVA with post-hoc Newman-Keuls test.

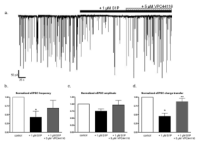

Figure 4.

S1P-induced suppression of sEPSC activity is attenuated by the $S1P_{1/3}$ receptor antagonist, VPC44116. **a**.) Whole-cell recording of sEPSCs from an individual cortical pyramidal neuron during the application of 1 μM S1P (black bar) and the subsequent addition of 5 μM VPC44116 (striped bar). The addition of VPC44116 partially attenuated the decrease in sEPSC frequency and amplitude induced by S1P. **b**.) sEPSC parameters for each condition were normalized to the pre-drug value in each neuron. 1 μM S1P decreased mean sEPSC frequency by 57.1± 16.7% (n=5, $p < 0.03$ vs. control) and the addition of 5 μM VPC44116 restored sEPSC frequency to 69.0 ± 21.6% of control frequency. **c**.) 1 μM S1P decreased mean median sEPSC amplitude by 25.0 ± 7.5% (n=5, $p > 0.05$ vs. control) and the addition of 5 μM VPC44116 restored sEPSC amplitude to 96.7 ± 15.8% of control amplitude. **d**.) 1 μM S1P decreased mean sEPSC charge transfer by 54.4 ± 9.1% (n=5, * $p < 0.002$ vs. control) and the addition of 5 μM VPC44116 restored sEPSC frequency to 87.3 ± 9.4% of control frequency (** $p < 0.01$ vs. S1P, $p > 0.05$ vs. control). Statistical significance was determined by ANOVA with post-hoc Newman-Keuls test.

NIH-PA Author Manuscript NIH-PA Author Manuscript NIH-PA Author Manuscript

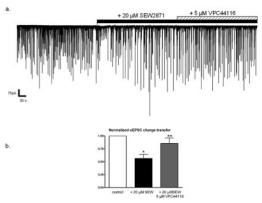

Figure 5.

The $S1P_1$ receptor agonist, SEW2871, decreases sEPSC activity. **a**.) Whole-cell recording of sEPSCs from an individual cortical pyramidal neuron during the application of 20 μM SEW2871 (black bar) and the subsequent addition of 5 μM VPC44116 (striped bar).**b**.) 20 μM SEW2871 decreased mean sEPSC charge transfer by 43.8 ± 8.2 % (n=8, * $p < 0.05$ vs. control by) and the administration of 5 μM VPC44116 in the continued presence of SEW2871 restored sEPSC charge transfer to 85.5 ± 10.1% of control values (n=8, ** $p<0.05$ vs. SEW2871 only, $p> 0.05$ vs. control). Statistical significance was determined by ANOVA with post-hoc Newman-Keuls test.

NIH-PA Author Manuscript NIH-PA Author Manuscript NIH-PA Author Manuscript

NIH-PA Author Manuscript

NIH-PA Author Manuscript

NIH-PA Author Manuscript

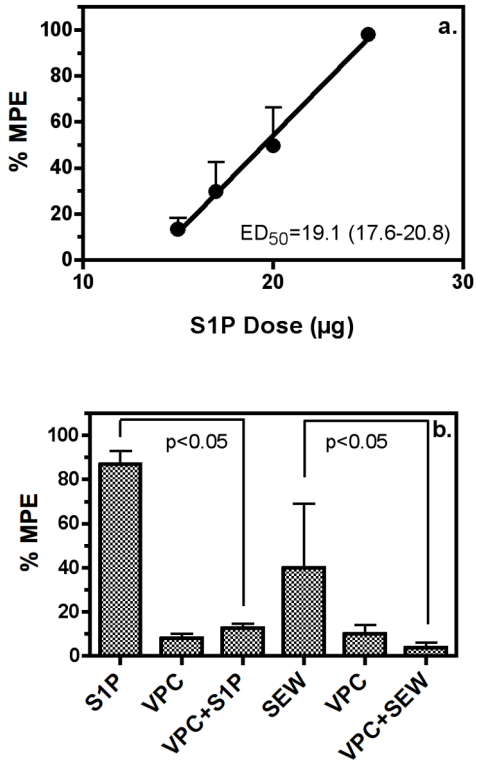

Figure 6.

S1P produces antinociception to thermal stimulus of the tail in mice via $S1P_1$ receptors. Mice were injected i.c.v with S1P with or without VPC44116. **a.** Dose-response curve for S1P-mediated antinociception in the tail-flick assay. S1P was injected i.c.v. and tail-flick latencies were obtained 20 min after injection. S1P produced dose-dependent antinociception. Data are mean %MPE values ± SEM. **b.** Antinociception expressed as mean %MPE ± SEM, determined following i.c.v. injection of S1P (25 μg) or the $S1P_1$-selective agonist SEW2871 (SEW, 50 μg) with or without prior injection (i.c.v.) of vehicle or the $S1P_{1/3}$ antagonist VPC44116 (25 μg). VPC44116 blocked the antinociceptive action of S1P or SEW2871, but administration of VPC44116 alone had no effect. Statistical significance of the data was determined by ANOVA with post-hoc Newman-Keuls test (n = 6).

NIH-PA Author Manuscript
NIH-PA Author Manuscript
NIH-PA Author Manuscript

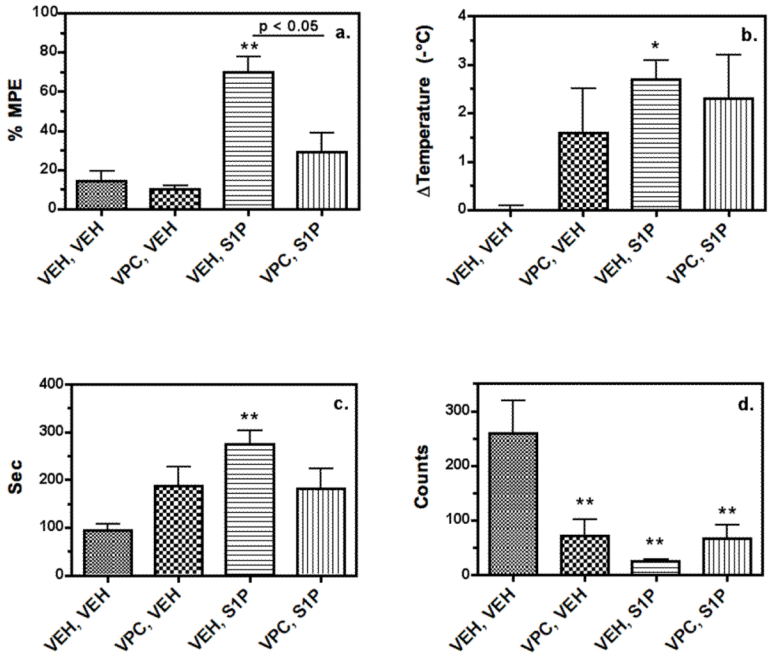

Figure 7.

S1P administered i.c.v. produces antinociception (a), hypothermia (b), catalepsy (c) and locomotor inhibition (d) in mice. Mice were injected (i.c.v.) with either vehicle or VPC44116 (25 μg) prior to injection (i.c.v.) with vehicle or S1P (25 μg), and tested following the final injection as described in Methods. S1P alone produced significant effects in all four tests. *, **, $p < 0.05$, 0.01 different from the vehicle/vehicle-treated group by ANOVA with post-hoc Dunnett's test (n = 6). VPC44116 significantly inhibited S1P-mediated antinociception (a.) as determined by ANOVA with post-hoc Newman-Keuls test (n = 6). VPC44116 alone produced catalepsy (d.) and partially inhibited S1P-induced locomotor inhibition (c.).

NIH-PA Author Manuscript

NIH-PA Author Manuscript

NIH-PA Author Manuscript

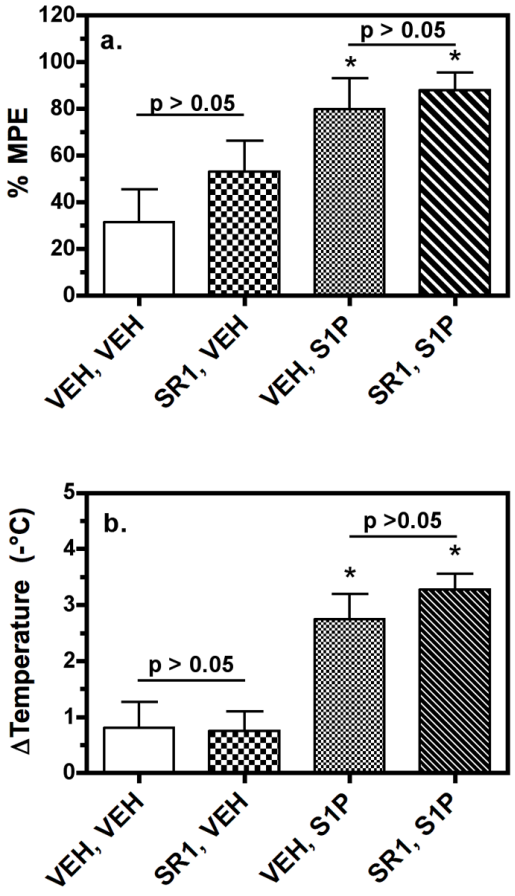

Figure 8.

S1P-mediated antinociception and hypothermia does not require cannabinoid CB_1 receptor activation. Mice were injected (i.p.) with 3mg/kg of the CB_1-selective antagonist rimonabant (SR141716A) prior to injection (i.c.v.) of S1P (25 μg), and tested following the final injection as described in Methods. S1P produced significant antinociception (a.) and hypothermia (b.). *, **, $p < 0.05$, 0.01 different from the vehicle/vehicle-treated group by ANOVA with post-hoc Dunnett's test (n = 6). Rimonabant did not inhibit S1P-induced antinociception (a.) or hypothermia (b.) and rimonabant alone had no significant effects on either measure (a., b.), as determined by ANOVA with post-hoc Newman-Keuls test (n = 6).